

Nonlinear dynamics of SWNTs. Energy beating and localization

Strozzi Matteo^{1*}, Manevitch Leonid I.², Smirnov Valeri V.², Pellicano Francesco³

Abstract

In this paper, the nonlinear vibrations and energy exchange of single-walled carbon nanotubes (SWNTs) are investigated. The Sanders-Koiter theory is applied to model the nonlinear dynamics of the system in the case of finite amplitude of vibration. The SWNT deformation is described in terms of longitudinal, circumferential and radial displacement fields. Simply supported boundary conditions are considered. The circumferential flexural modes (CFMs), radial breathing modes (RBMs) and beam-like modes (BLMs) are studied. A numerical model of the SWNT dynamics is proposed. The three displacement fields are expanded in the nonlinear field by using approximate linear eigenfunctions. An energy method based on the Lagrange equations is used to reduce the nonlinear partial differential equations of motion to a set of nonlinear ordinary differential equations, which is solved using the implicit Runge-Kutta numerical method. The nonlinear energy exchange along the SWNT axis is analysed for different initial excitation amplitudes. The internal resonances between CFMs, RBMs and BLMs are investigated. The transition from energy beating to energy localization in the nonlinear field is studied.

Keywords

Nonlinear dynamics, energy exchange, SWNTs

¹ Department of Engineering, University of Ferrara, Ferrara, Italy

² N.N. Semenov Institute of Chemical Physics, Russian Academy of Sciences RAS, Moscow, Russia

³ Department of Engineering "Enzo Ferrari", University of Modena and Reggio Emilia, Modena, Italy

* Corresponding author: matteo.strozzi@unimore.it

Introduction

In this paper, we are going to study the problems of energy exchange and localization along the SWNT axis by considering appropriate parameters and models, where energy transfer and spatially localized excitations represent very interesting phenomena in the nonlinear dynamics of solids and structures [1-2]. The analogies between continuous shells and discrete SWNTs led to large application of the elastic shell theories for the SWNT structural analysis [3-10].

In this paper, the discrete SWNTs are modelled as continuum elastic thin circular cylindrical shells considering equivalent mechanical parameters. The nonlinear dynamics of the SWNT is studied by applying the Sanders-Koiter nonlinear thin shell theory. An energy method based on the Lagrange equations is used to reduce the nonlinear partial differential equations of motion to a set of nonlinear ordinary differential equations, which is solved using the implicit Runge-Kutta numerical method.

The nonlinear energy exchange along the axis of a simply supported SWNT is analysed for different amplitudes of initial excitation. The internal resonances between CFMs, RBMs and BLMs are considered. The transition from energy beating to energy localization in nonlinear field is studied.

1. Sanders-Koiter nonlinear shell theory

In Figure 1, a circular cylindrical shell having radius R , length L and thickness h is represented; a cylindrical coordinate system $(O; x, \theta, z)$ is considered, where the origin O of the reference system is located at the centre of one end of the cylindrical shell.

In Figure 1, three displacement fields are represented: longitudinal $u(x, \theta, t)$, circumferential $v(x, \theta, t)$ and radial $w(x, \theta, t)$; the radial displacement field w is considered positive outward; (x, θ) are the longitudinal and angular coordinates of an arbitrary point on the middle surface of the shell; z is the radial coordinate along the thickness h ; t is the time.

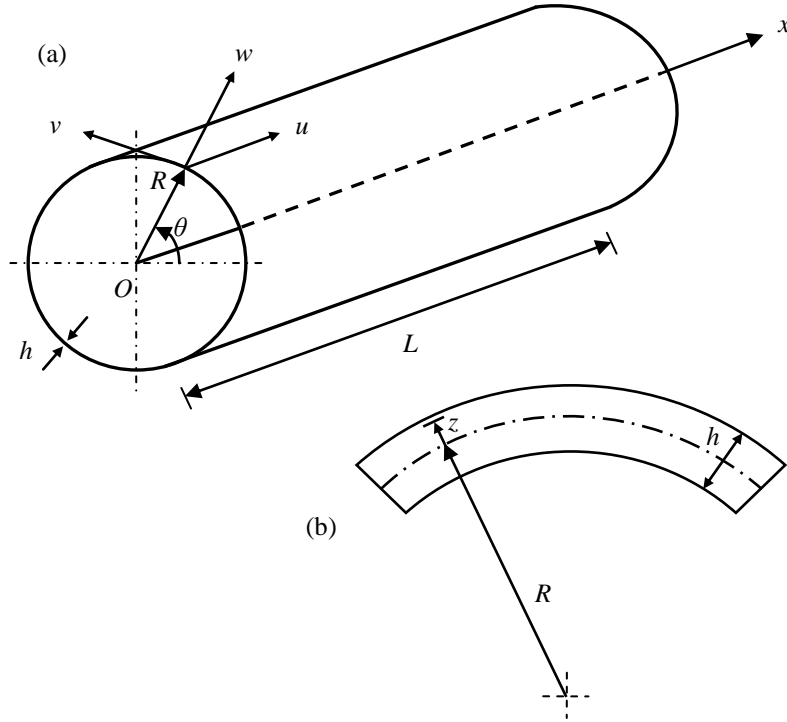


Figure 1. Geometry of the cylindrical shell. (a) Complete shell; (b) cross-section of the shell surface.

1.1 Displacement fields and strain-displacement relationships

The nondimensional displacement fields $(\tilde{u}, \tilde{v}, \tilde{w})$ can be written in the following form [5]

$$\tilde{u} = \frac{u}{R} \quad \tilde{v} = \frac{v}{R} \quad \tilde{w} = \frac{w}{R} \quad (1)$$

where (u, v, w) are the dimensional displacement fields and R is the radius of the shell.

The nondimensional middle surface strains of the shell $(\tilde{\varepsilon}_{x,0}, \tilde{\varepsilon}_{\theta,0}, \tilde{\gamma}_{x\theta,0})$ are expressed as [8]

$$\tilde{\varepsilon}_{x,0} = \alpha \frac{\partial \tilde{u}}{\partial \eta} + \frac{1}{2} \alpha^2 \left(\frac{\partial \tilde{w}}{\partial \eta} \right)^2 + \frac{1}{8} \left(\alpha \frac{\partial \tilde{v}}{\partial \eta} - \frac{\partial \tilde{u}}{\partial \theta} \right)^2 \quad (2)$$

$$\tilde{\varepsilon}_{\theta,0} = \frac{\partial \tilde{v}}{\partial \theta} + \tilde{w} + \frac{1}{2} \left(\frac{\partial \tilde{w}}{\partial \theta} - \tilde{v} \right)^2 + \frac{1}{8} \left(\frac{\partial \tilde{u}}{\partial \theta} - \alpha \frac{\partial \tilde{v}}{\partial \eta} \right)^2 \quad (3)$$

$$\tilde{\gamma}_{x\theta,0} = \frac{\partial \tilde{u}}{\partial \theta} + \alpha \frac{\partial \tilde{v}}{\partial \eta} + \alpha \frac{\partial \tilde{w}}{\partial \eta} \left(\frac{\partial \tilde{w}}{\partial \theta} - \tilde{v} \right) \quad (4)$$

where $\eta = x/L$ is the nondimensional longitudinal coordinate of the shell and $\alpha = R/L$.

The nondimensional middle surface changes in curvature and torsion $(\tilde{k}_x, \tilde{k}_\theta, \tilde{k}_{x\theta})$ are [8]

$$\tilde{k}_x = -\alpha^2 \frac{\partial^2 \tilde{w}}{\partial \eta^2} \quad \tilde{k}_\theta = \frac{\partial \tilde{v}}{\partial \theta} - \frac{\partial^2 \tilde{w}}{\partial \theta^2} \quad \tilde{k}_{x\theta} = -2\alpha \frac{\partial^2 \tilde{w}}{\partial \eta \partial \theta} + \frac{3}{2} \alpha \frac{\partial \tilde{v}}{\partial \eta} - \frac{1}{2} \frac{\partial \tilde{u}}{\partial \theta} \quad (5)$$

1.2 Elastic strain and kinetic energy

The nondimensional elastic strain energy \tilde{E} of a cylindrical shell is expressed as follows [5]

$$\tilde{E} = \frac{1}{2} \frac{1}{(1-\nu^2)} \left\{ \int_0^1 \int_0^{2\pi} \left[\tilde{\varepsilon}_{x,0}^2 + \tilde{\varepsilon}_{\theta,0}^2 + 2\nu \tilde{\varepsilon}_{x,0} \tilde{\varepsilon}_{\theta,0} + \frac{(1-\nu)}{2} \tilde{\gamma}_{x\theta,0}^2 \right] d\eta d\theta + \frac{\beta^2}{12} \int_0^1 \int_0^{2\pi} \left[\tilde{k}_x^2 + \tilde{k}_\theta^2 + 2\nu \tilde{k}_x \tilde{k}_\theta + \frac{(1-\nu)}{2} \tilde{k}_{x\theta}^2 \right] d\eta d\theta \right\} \quad (6)$$

with $\beta = h/R$.

The nondimensional velocity fields $(\tilde{u}', \tilde{v}', \tilde{w}')$ are obtained from the dimensional displacement fields $(\tilde{u}, \tilde{v}, \tilde{w})$ and the nondimensional time τ in the following form [5]

$$\tilde{u}' = \frac{d\tilde{u}}{d\tau} \quad \tilde{v}' = \frac{d\tilde{v}}{d\tau} \quad \tilde{w}' = \frac{d\tilde{w}}{d\tau} \quad (7)$$

The nondimensional kinetic energy \tilde{T} of a cylindrical shell is given by [5]

$$\tilde{T} = \frac{1}{2} \gamma \int_0^1 \int_0^{2\pi} (\tilde{u}'^2 + \tilde{v}'^2 + \tilde{w}'^2) d\eta d\theta \quad (8)$$

where $\gamma = \rho R^2 \omega_0^2 / E$.

2. Numerical solution of the Sanders-Koiter nonlinear shell theory

In order to obtain a numerical solution of the SWNT nonlinear dynamics, a two-steps procedure is used: i) the three displacement fields are expanded using approximated eigenfunctions obtained in linear field; ii) the Lagrange equations are considered in conjunction with the nonlinear elastic strain energy in order to obtain a set of nonlinear ordinary differential equations of motion.

2.1 Nonlinear vibration analysis

In the nonlinear analysis, the full expression of the nondimensional elastic strain energy (6), which contains terms up to the fourth order (cubic nonlinearity), is considered.

The three displacement fields $\tilde{u}(\eta, \theta, \tau)$, $\tilde{v}(\eta, \theta, \tau)$, $\tilde{w}(\eta, \theta, \tau)$ are expanded in the form [10]

$$\begin{aligned} \tilde{u}(\eta, \theta, \tau) &= \sum_{j=1}^{N_u} \sum_{n=1}^N \tilde{U}^{(j,n)}(\eta, \theta) \tilde{f}_{u,j,n}(\tau) \\ \tilde{v}(\eta, \theta, \tau) &= \sum_{j=1}^{N_v} \sum_{n=1}^N \tilde{V}^{(j,n)}(\eta, \theta) \tilde{f}_{v,j,n}(\tau) \\ \tilde{w}(\eta, \theta, \tau) &= \sum_{j=1}^{N_w} \sum_{n=1}^N \tilde{W}^{(j,n)}(\eta, \theta) \tilde{f}_{w,j,n}(\tau) \end{aligned} \quad (9)$$

where $\tilde{U}^{(j,n)}(\eta, \theta)$, $\tilde{V}^{(j,n)}(\eta, \theta)$, $\tilde{W}^{(j,n)}(\eta, \theta)$ are linear mode shapes and $(\tilde{f}_{u,j,n}(\tau), \tilde{f}_{v,j,n}(\tau), \tilde{f}_{w,j,n}(\tau))$ are unknown time laws (step i).

2.2 Lagrange equations

Expansions (9) are inserted into the expressions of elastic strain energy (6) and kinetic energy (8); the nondimensional Lagrange equations of motion for free vibrations can be expressed as [10]

$$\frac{d}{d\tau} \left(\frac{\partial \tilde{T}}{\partial \tilde{q}_i'} \right) + \frac{\partial \tilde{E}}{\partial \tilde{q}_i} = 0 \quad i \in [1, N_{\max}] \quad (10)$$

where the maximum number of degrees of freedom N_{\max} depends on the number of vibration modes considered in the expansions (10).

The nondimensional lagrangian coordinates $(\tilde{q}_i, \tilde{q}'_i)$ can be written in the form [10]

$$\tilde{q}_i = \frac{q_i}{R} \qquad \tilde{q}'_i = \frac{d\tilde{q}_i}{d\tau} \qquad i \in [1, N_{\max}] \qquad (11)$$

where the nondimensional lagrangian coordinates \tilde{q}_i correspond to the previous nondimensional modal coordinates $(\tilde{f}_{u,j,n}(\tau), \tilde{f}_{v,j,n}(\tau), \tilde{f}_{w,j,n}(\tau))$.

Substituting the vector functions $\tilde{F}(\tilde{q}_i) = \partial\tilde{E}/\partial\tilde{q}_i$ and $\tilde{M}\tilde{q}_i'' = d(\partial\tilde{T}/\partial\tilde{q}'_i)/d\tau$ into equation (10), where \tilde{M} denotes the mass matrix, we obtain [10]

$$\tilde{M}\tilde{q}_i'' + \tilde{F}(\tilde{q}_i) = 0 \qquad i \in [1, N_{\max}] \qquad (12)$$

Inserting the vector function $\tilde{F}_{x,i} = \tilde{M}^{-1}\tilde{F}(\tilde{q}_i)$ in equation (12), the nondimensional Lagrange equations of motion for free vibrations can be expressed in the following form [10]

$$\tilde{q}_i'' + \tilde{F}_{x,i} = 0 \qquad i \in [1, N_{\max}] \qquad (13)$$

By using the Lagrange equations (13), a set of nonlinear ordinary differential equations is found (step ii), which is solved numerically by applying the implicit Runge-Kutta method.

3. Numerical results

In this section, the nonlinear energy exchange along the axis of a simply supported SWNT is analysed. The dynamical system is conservative (no damping); as initial condition, a localized energy in one half of the SWNT axis is given, and then it is checked if the energy remains localized; different initial excitation amplitudes are considered; the internal resonances between circumferential flexural modes (CFMs), radial breathing modes (RBMs) and beam-like modes (BLMs) are studied.

3.1 Circumferential flexural modes ($n = 2$)

The energy localization is a strongly nonlinear phenomenon, which depends on the amount of the energy provided to the SWNT. When the initial energy is quite small, a resonant interaction of two CFMs having close frequencies takes place and the initial localized energy is immediately destroyed, with a periodic redistribution of the energy between the two halves along the SWNT axis in the time.

This process can be interpreted as the beating between two particles, each one containing about one half of the SWNT axis: in the case of small amplitude initial energy, a periodic energy exchange between the two halves of the SWNT takes place.

When the amplitude of the initial energy is large enough, the nonlinearity preserves the energy localization in the initially excited part of the SWNT. The nonlinear oscillations of the SWNT become localized ones if the amplitude of the initial energy exceeds a threshold, which depends on the SWNT length. This energy localization is due to the intensive nonlinear resonant interaction between the two CFMs. The initial excitation amplitude corresponding to the transition from energy beating to energy confinement in one half of the SWNT axis is called “energy localization threshold” [10].

In Figure 2, the time evolution of the energy distribution along the axis of a simply supported SWNT is reported, the aspect ratio is $L/R = 20$, the natural frequencies of the two resonant CFMs (1,2) and (2,2) are $f_{1,2} = 0.29317$ THz and $f_{2,2} = 0.31165$ THz, respectively, with $f_{2,2}/f_{1,2} = 1.063$ (1:1 internal resonance): for this specific SWNT, the energy localization threshold is equal to $X(0)_{\text{loc}} = 0.14593$.

In Figure 2(a), the initial excitation amplitude is $X(0) = 0.080$ (lower than the energy threshold), and a periodic energy exchange between the two halves of the SWNT axis takes place. The initial excitation domain ($\tau = 0$) corresponds to the second half of the SWNT axis ($0.5 \leq \eta \leq 1$) (localized initial energy): the time evolution shows that the localization is promptly lost and the energy spreads on the first half of the SWNT axis ($0 \leq \eta \leq 0.5$).

In Figure 2(b), the initial excitation amplitude is equal to $X(0) = 0.160$ (higher than the energy threshold), and an energy localization in the second half of the SWNT axis (initial excitation domain) is given; in this case, the time evolution shows that the energy never flows toward the first half of the SWNT axis, and a perfect energy confinement is manifested.

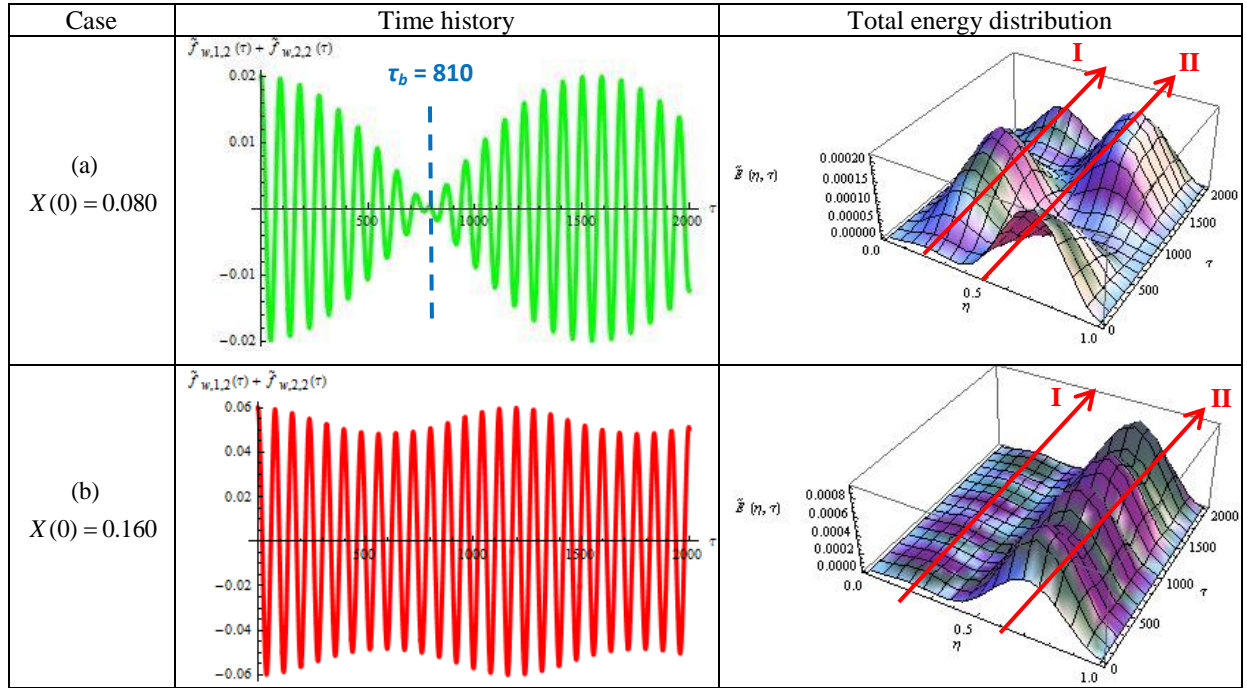


Figure 2. Time evolution of the total energy distribution along the axis of a simply supported SWNT; $L/R = 20$; resonant CFMs (1,2),(2,2); energy localization threshold $X(0) = 0.14593$. (a) Initial excitation amplitude $X(0) = 0.080$ (energy beating). (b) Initial excitation amplitude $X(0) = 0.160$ (energy localization).

3.2 Radial breathing modes ($n = 0$)

In the case of small amplitude initial energy, a weak resonant interaction of two RBMs having close frequencies takes place, the initial localized energy is immediately destroyed and a periodic energy exchange between the two halves of the SWNT axis arises. The time scale of this periodic energy redistribution is inversely proportional to the natural frequencies difference of the RBMs.

When the amplitude of the initial energy increases, a strong resonant interaction of the two excited RBMs takes place and the effect of the nonlinearity increases; again, the initial localized energy is immediately destroyed and a periodic energy exchange between the two halves of the SWNT axis is present, with the same time scale of the previous small amplitude initial energy case.

In the case of the RBMs (differently from the CFMs), the nonlinear oscillations do not become localized ones for any amplitude of the initial excitation energy and a periodic energy exchange between the two halves of the SWNT axis is always present, where the time period of the nonlinear energy beating is not dependent on the initial excitation amplitude.

In Figure 3, the time evolution of the energy distribution along the axis of a simply supported SWNT is reported, the aspect ratio is $L/R = 20$, different initial excitation amplitudes are considered, the initial excitation domain ($\tau = 0$) corresponds to the second half of the SWNT axis ($0.5 \leq \eta \leq 1$) (localized initial energy), the natural frequencies of the two resonant RBMs (1,0) and (2,0) are $f_{1,0} = 4.47371$ THz and $f_{2,0} = 4.48048$ THz, respectively, with $f_{2,0}/f_{1,0} = 1.001$ (1:1 internal resonance): for this specific SWNT, the nonlinear energy localization phenomenon is not present.

In Figure 3(a), the small initial excitation amplitude $X(0) = 0.050$ is given (weak interaction of the RBMs), and a periodic weakly nonlinear energy exchange between the two halves of the SWNT axis arises (low peak of total energy distribution), with energy beating period τ_b .

In Figure 3(b), the high initial excitation amplitude $X(0) = 0.200$ is applied (strong interaction of the RBMs), and a periodic strongly nonlinear energy exchange between the two halves of the SWNT axis is given (high peak of energy distribution), with the same energy beating period of Figure 3(a).

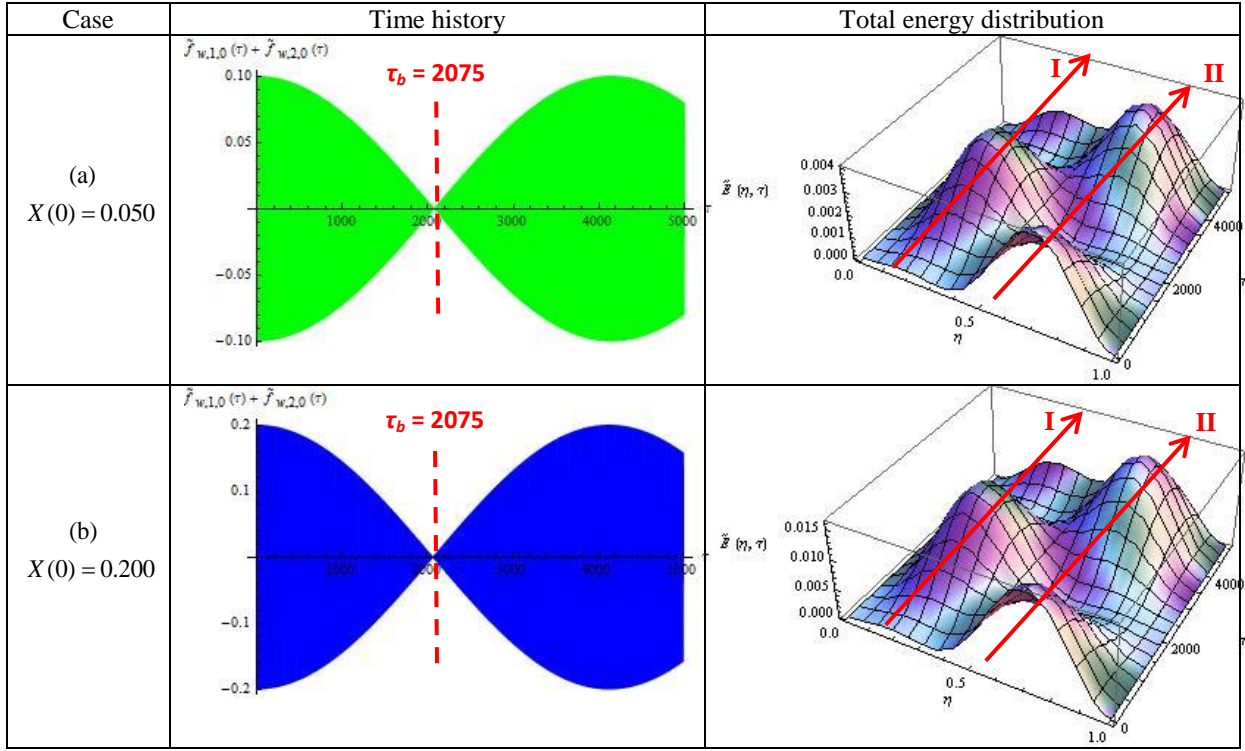


Figure 3. Time evolution of the total energy distribution along the axis of a simply supported SWNT; $L/R = 20$; resonant RBMs (1,0),(2,0); nonlinear energy beating period $\tau_b = 2075$. (a) Initial excitation amplitude $X(0) = 0.050$ (energy beating). (b) Initial excitation amplitude $X(0) = 0.200$ (energy beating).

From the previous numerical analyses for the RBMs nonlinear oscillations it was found that, for any amplitude of initial excitation, the initial energy localization in the second part of the SWNT axis is promptly lost, and a periodic energy exchange between the two halves of the SWNT axis arises, where the nonlinear energy beating period τ_b is not dependent on the initial excitation amplitude.

3.3 Internal resonance between beam-like ($n = 1$) and circumferential flexural ($n = 2$) modes

In the case of small amplitude initial energy, a weak resonant interaction between a BLM and a CFM with $m = 3$ longitudinal half-waves having close frequencies takes place, the initial localized energy is destroyed and a periodic energy distribution along the three parts of the SWNT axis arises.

When the amplitude of the initial energy increases, a strong resonant interaction between the two excited BLM and CFM takes place and the effect of the nonlinearity increases; again, the initial localized energy is immediately destroyed and a periodic energy distribution along the three parts of the SWNT axis is present, where the time scale of this periodic energy distribution is lower than the time scale of the small amplitude initial energy configuration.

In the case of internal resonance between BLM and CFM with three longitudinal half-waves, the nonlinear oscillations do not become localized ones for any amplitude of the initial excitation energy and a periodic energy distribution along the three parts of the SWNT axis is always present, where the time period of the energy redistribution τ_r is dependent on the initial excitation amplitude.

In Figure 4, the time evolution of the energy distribution along the axis of a simply supported SWNT is reported, the aspect ratio is $L/R = 30$, different initial excitation amplitudes are considered, the initial excitation domain ($\tau = 0$) corresponds to the three parts of the SWNT axis ($0.1 \leq \eta \leq 0.3$, $0.4 \leq \eta \leq 0.6$, $0.7 \leq \eta \leq 0.9$) (localized initial energy), the natural frequencies of the resonant BLM (3,1) and CFM (3,2) are $f_{3,1} = 0.06109$ THz and $f_{3,2} = 0.06969$ THz, respectively, with $f_{3,2}/f_{3,1} = 1.141$ (1:1 internal resonance): for this SWNT, the nonlinear energy localization is not present.

In Figure 4(a), the small initial excitation $X(0) = 0.020$ is given (weak interaction of BLM and CFM), and a periodic weakly nonlinear energy distribution along the three parts of the SWNT axis arises (low peak of total energy distribution).

In Figure 4(b), the high initial excitation $X(0) = 0.050$ is given (strong interaction of BLM and CFM), and a periodic strongly nonlinear energy distribution along the three parts of the SWNT axis is given (high peak of energy distribution), with a lower energy redistribution period τ_r , than Figure 4(a).

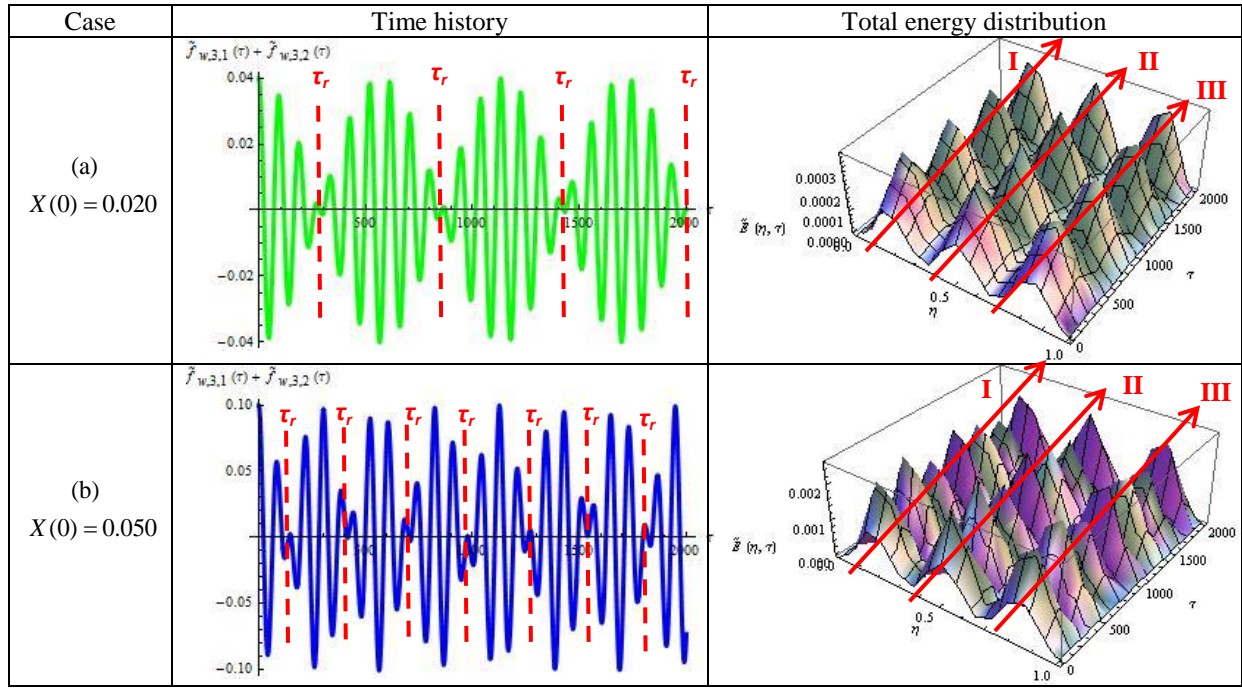


Figure 4. Time evolution of the total energy distribution along the axis of a simply supported SWNT; $L/R = 30$; internal resonance between the BLM (3,1) and the CFM (3,2); nonlinear energy redistribution period τ_r .
(a) Initial excitation amplitude $X(0) = 0.020$. (b) Initial excitation amplitude $X(0) = 0.050$.

Conclusions

In this paper, the nonlinear vibrations and energy exchange of SWNTs are studied by using the Sanders-Koiter shell theory. Simply supported boundary conditions are applied. The circumferential flexural modes (CFMs), radial breathing modes (RBMs) and beam-like modes (BLMs) are analysed. The nonlinear energy exchange along the SWNT axis is considered for different initial excitation amplitudes. The transition from energy beating to energy localization in nonlinear field is evaluated.

In the case of two resonant CFMs, the energy localization phenomenon is present. An initial excitation amplitude lower than the energy localization threshold gives a periodic energy exchange between the two halves of the SWNT axis (energy beating). Conversely an initial excitation amplitude higher than the energy threshold gives an energy localization in one half of the SWNT axis (initial excitation domain) and a perfect energy confinement is manifested (energy localization).

In the case of two resonant RBMs, the energy localization phenomenon is not present. A small initial excitation amplitude (weak interaction of the RBMs) gives a periodic weakly nonlinear energy exchange between the two halves of the SWNT axis (low peak of total energy distribution). Similarly, a high initial excitation amplitude (strong interaction of the RBMs) gives a periodic strongly nonlinear energy exchange between the two halves of the SWNT axis (high peak of energy distribution) with the same energy beating period of the small initial excitation amplitude case. Therefore, for the RBMs nonlinear oscillations it was found that, for any amplitude of initial excitation, the initial energy localization is lost, and a periodic energy exchange between the two halves of the SWNT axis arises, where the nonlinear energy beating period is not dependent on the initial excitation amplitude.

In case of internal resonance between a BLM and a CFM with three longitudinal half-waves, the energy localization phenomenon is again not present. A small amplitude initial energy gives a weak resonant interaction between the BLM and the CFM, the initial localized energy is destroyed and a periodic energy distribution along the three parts of the SWNT axis arises. When the amplitude of the initial energy increases, a strong resonant interaction between the two excited BLM and CFM takes place and the effect of the nonlinearity increases; again, the initial localized energy is immediately destroyed and a periodic energy distribution along the three parts of the SWNT axis is present, where the time scale of this periodic energy distribution is lower than the time scale of the small amplitude initial energy configuration.

References

- [1] Manevitch L.I., Gendelman O.V. *Tractable Models of Solid Mechanics. Formulation, Analysis and Interpretation*. Berlin: Springer-Verlag; 2011.
- [2] Vakakis A.F., Manevitch L.I., Mikhlin Y.V., Pilipchuk V.N., Zevin A.A. *Normal Modes and Localization in Nonlinear Systems*. New York: Wiley; 1996.
- [3] Liew K.M., Wang Q. Analysis of wave propagation in carbon nanotubes via elastic shell theories. *International Journal of Engineering Science*, 2007, Vol. 45, p. 227-241.
- [4] Wang C.Y., Ru C.Q., Mioduchowski A. Applicability and Limitations of Simplified Elastic Shell Equations for Carbon Nanotubes. *Journal of Applied Mechanics*, 2004, Vol. 71, p. 622-631.
- [5] Strozzi M., Manevitch L.I., Pellicano F., Smirnov V.V., Shepelev D.S. Low-frequency linear vibrations of single-walled carbon nanotubes: analytical and numerical models. *Journal of Sound and Vibration*, 2014, Vol. 333, p. 2936-2957.
- [6] Wang L., Hu H. Flexural wave propagation in single-walled carbon nanotubes. *Physical Review B*, 2005, Vol. 71, p. 195412 (7).
- [7] Batra R.C., Gupta S.S. Wall Thickness and Radial Breathing Modes of Single-Walled Carbon Nanotubes. *Journal of Applied Mechanics*, 2008, Vol. 75, p. 061010 (6).
- [8] Smirnov V.V., Manevitch L.I., Strozzi M., Pellicano F. Nonlinear optical vibrations of single-walled carbon nanotubes. 1. Energy exchange and localization of low-frequency oscillations. *Physica D*, 2016, Vol. 325, p. 113-125.
- [9] Chang T. A molecular based anisotropic shell model for single-walled carbon nanotubes. *Journal of the Mechanics and Physics of Solids*, 2010, Vol. 58, p. 1422-1433.
- [10] Strozzi M., Smirnov V.V., Manevitch L.I., Milani M., Pellicano F. Nonlinear vibrations and energy exchange of single-walled carbon nanotubes. Circumferential flexural modes. *Journal of Sound and Vibration*, 2016, Vol. 381, p. 156-178.